



Eco-friendly method for reclaimed silicon wafer from photovoltaic module: from separation to cell fabrication

Journal:	<i>Green Chemistry</i>
Manuscript ID	GC-ART-08-2015-001819.R2
Article Type:	Paper
Date Submitted by the Author:	02-Nov-2015
Complete List of Authors:	Park, Jongsung; University of New South Wales, Photovoltaic and Renewable Energy Engineering Kim, Wangou; Korea Interfacial Science and Engineering Institute, Cho, Namjun; Korea Univ. of Tech. & Edu. Lee, Haksoo; Korea Interfacial Science and Engineering Institute, Park, Nochang; Korea Electronics Technology Institute,



Green Chemistry

ARTICLE

Eco-friendly method for reclaimed silicon wafer from photovoltaic module: from separation to cell fabrication

Jongsung Park^b, Wangou Kim^c, Namjun Cho^d, Haksoo Lee^{c*} and Nochang Park^{a*}

Received 00th January 20xx,
Accepted 00th January 20xx

DOI: 10.1039/x0xx00000x

www.rsc.org/

A sustainable method for reclaiming silicon (Si) wafer from an end-of-life photovoltaic module is examined in this paper. A thermal process was employed to remove ethylene vinyl acetate and the back-sheet. We found that a ramp-up rate of 15 °C/min and an annealing temperature of 480 °C enabled recovery of the undamaged wafer from the module. An ecofriendly process to remove impurities from the cell surface was developed. We also developed an etching process that precludes the use of hydrofluoric (HF) acid. The method for removing impurities consists of three steps: (1) recovery of the silver (Ag) electrode using nitric acid (HNO₃); (2) mechanical removal of the anti-reflecting coating, emitter layer, and p–n junction simultaneously; and (3) removal of the aluminum (Al) electrode using potassium hydroxide (KOH). The reclaimed wafers showed properties that are almost identical to those of commercial virgin wafers: 180 μm average thickness; 0.5 and 3.7 Ω•cm minimum and maximum resistivities, respectively; and 1.69 μs average carrier lifetime. In addition, cells fabricated with the reclaimed wafers showed an efficiency equivalent to that of the initial cells.

Introduction

Photovoltaic (PV) energy now holds an important position in the renewable-energy market. The annual PV installation around the world in 2014 is 38.7 GW.¹ More than 10 GW connected to the grid for PV in the EU in 2013.² PV installation is greater than that from fossil fuel (7.5 GW) and coal (1.9 GW).² With the growing number of installations for PV systems and the limited availability of resources, the end-of-life (EoL) management of PV modules is becoming increasingly urgent.³ Proper EoL management of PV modules offers a sustainable solution to problems of resource availability, economic feasibility, and EoL environmental risks.⁴ The cumulative amount of PV waste in 2017 is estimated to be 870 tons, and the total amount of PV waste is estimated to increase by 1,957,099 tons in 2038.⁵ These numbers make the management of waste electrical and electronic equipment

(WEEE) toward sustainability an interesting challenge.⁶ The recent decision made by the EU Commission to include PV panels in the new WEEE directive follows these expectations, in an effort to limit the negative impacts.⁷ On the basis of this principle, PV manufacturers, and distributors have the legal obligation to ensure take-back and recycling of their discarded products within European borders.⁸ PV modules contain valuable metals such as silver, copper, tin, and the hazardous material, lead.⁹ Lead causes serious illnesses in humans because of its toxicity.^{9,10} Accordingly, it is also important to remove lead in PV modules although it is exempted from the regulation for hazardous substances. Since the industry needs to continue reducing the price of PV module for it to be sustainable in a competitive PV market, the cost of compliance must be minimized.¹¹ This requires the optimization of both material recovery and reclamation of wafers. Metals may be recovered by using the current technologies.^{11,12,13}

Recycling can ensure the sustainability of the supply chain in the long term^{14,15} by enhancing the recovery of energy and materials embedded in PV modules and by reducing CO₂ emissions, energy payback time (EPBT), and greenhouse-gas payback time related to the manufacture of PV modules.¹⁶

The average price of polysilicon (p-Si) is approximately \$20/kg in January 2014.¹⁷ The drop in its price has stopped because of increasing demand; prices have even increased slightly compared with those in January 2013.¹⁷ This increase resulted in changes to the different cost elements in module

^a Robust Components and System Research Centre, Korea Electronics Technology Institute, Seong-Nam, Republic of Korea.

^b School of Photovoltaic and Renewable Energy Engineering, University of New South Wales(UNSW), Sydney, NSW 2052, Australia.

^c Korea Interfacial Science and Engineering Institute, Cheonan, Republic of Korea.

^d School of Energy Materials & Chemical Engineering, Korea Univ. of Tech. & Edu., Cheonan, Republic of Korea.

† Footnotes relating to the title and/or authors should appear here. Electronic Supplementary Information (ESI) available: [details of any supplementary information available should be included here]. See DOI: 10.1039/x0xx00000x

production. This is a drawback for module manufacturing, because it increases the pressure to reduce the cost further. p-Si and wafers remain the most expensive materials in modules.¹⁷ p-Si and wafers have a significant impact on the total price, with the module-conversion price share comprising over 30%. Recycling technology of PV modules can reduce the manufacturing cost by enabling the use of reclaimed wafers,^{9, 18} which can reduce the energy consumption in Si purification and wafer manufacture. Reclaimed wafers may be obtained from EOL modules as a type of broken or unbroken wafers. Broken wafers are crushed into powder form used for ingot production¹⁹ or are applied as a biogenic silica source for ashing of rice hulls.²⁰ In order to be used for solar cells, broken wafers are normally refined into semiconductor feedstock of over 99.9999% purity through the Siemens process, which is estimated to account for 75% of the total production energy for crystalline Si PV modules.²¹ However, this refining process is not necessary for achieving minimum purity for unbroken wafers. Instead, they require a process for removing impurities remaining on the wafer surface, such as the metal electrode, anti-reflection coating (ARC), and p–n junction. To remove such impurities, hydrofluoric (HF) acid treatment,²² which is harmful to humans and to the environment, is used. Consequently, development of a process that does not use HF is one of the motivations behind the present study.

The use of reclaimed wafer enables reduction of the EPBT of PV modules. Through calculations, M.J. de Wild-Scholten²³ found that the EPBT for a mono-Si PV system for a commercial rooftop PV is 1.96 year. Processes that contribute to the EPBT consist of production of silicon feedstock, ingot, wafer, cell, module, mounting, and inverter. Among these processes, those for feedstock, ingot, and wafer contribute over 60% to the EPBT. If the energy for these processes is reduced by using reclaimed wafer, then the EPBT can be significantly reduced to less than 1.96 years. Energy consumption is also closely related to the manufacturing cost. In their calculation of the EPBT of PV modules containing recycled materials, M. Goe et al.²⁴ found that the EPBT decreases as the recycling rate increases at a given module efficiency. In general, a 3–5% change in the recycling rate produces a reduction in EPBT equivalent to a 1% change in module efficiency. Therefore, exhaustive recovery of Si materials has the potential of reducing the module cost and EPBT.

In order to evaluate the economic feasibility of PV recycling, Choi et al.⁴ developed mathematical models to analyze the profitability of recycling technologies and to guide tactical decisions for optimal location of PV take-back centers necessary for the collection of EoL products. Their results show that the market price of the reclaimed materials is an important factor in the profitability of the recycling process. They illustrate the importance of recovering glass and expensive metals from PV modules. As of 2011, the average market price of glass, aluminum (Al), copper (Cu), and Si are estimated to be \$0.07/kg, \$2/kg, \$7/kg, and \$2.5/kg respectively.⁴ However, that of reclaimed wafer is estimated to be \$35/kg (assuming 22.7 g/wafer and \$0.8/wafer). These results indicate that reclaimed wafers are more valuable than

the other materials are. The following technologies are required to recycle PV modules^{9, 18, 22, 25–28}:

- (1) Recovery of glass and metals such as Ag, Al, Cu, Pb, and Sn
- (2) Recovery of broken wafers
- (3) Glass–ethylene vinyl acetate (EVA)/EVA cell separation
- (4) Recovery of unbroken wafers and technologies for the removal of impurities such as the metal electrode, AR coating, and p–n junction.

Kang et al.⁹ reported a procedure for recovering Si and glass. They used toluene for glass recovery. The sample was immersed in organic solvent at 90 °C for about 2 days. They recovered Si by using H₂O, HF (acid concentration: 48%), HNO₃ (70%), H₂SO₄ (97%), and CH₃COOH (99%). The results show that a high yield of silicon with 99.999% purity could be obtained.

G. Granata et al.²⁵ investigated the recycling of broken wafers by physical operation, which consists of crushing by two rotors, thermal treatment, crushing by two rotors, and hammer crushing.

A method to thermally remove components in glass–EVA/EVA cell separation was developed in 1998 by the research group of Frisson.²⁶ Similarly, E. Klugmann-Radziemska et al.²⁷ performed glass–polymer separation by using a thermal process. However, the thermal process is not discussed in detail in their paper. From the thermal process, they obtained unbroken wafers, which were used to produce new silicon solar cells. Despite that they have no SiN_x ARC, the new cells have very good energy conversion efficiency (13–15%). Frisson et al.²⁶ also fabricated solar cells using reclaimed wafers. They obtained the same results for reclaimed and virgin wafers (around 16%).

To achieve the required purity of the reclaimed wafers, conditions for chemical treatment need to be precisely adjusted. To this end, L. Frisson et al.²² used 15% hydrofluoric (HF) acid treatment followed by treatment with a 4:1 H₂SO₄/H₂O₂ solution at 80 °C. E. Klugmann-Radziemska et al.²⁸ used 83.33 ml of HNO₃ (65%), 50 ml of HF (40%), 50 ml of CH₃COOH (99.5%), and 1 ml of Br₂ within the range of 70–80 °C.

Existing remanufacturing processes are based on chemical etching, an industrially feasible approach that provides low technical barriers for startup. However, these methods require multilevel chemical processes and special equipment for chemicals such as HF and fluorosilicic acid.²⁸ These chemicals are also harmful to humans and to the environment. Methods for removing impurities without the use of such toxic chemicals have not been reported yet, as summarized in Table 1.

The objectives of the research reported here were to: (1) avoid the use of hazardous substance such as HF, (2) reduce the usage of chemicals such as HNO₃, H₃PO₄, and (3) develop a low cost, low energy process for Si wafer by the use of reclaimed wafer. In the present study, we focused on module separating methods based on a thermal process to obtain unbroken wafers from a PV module. The effects of annealing temperature and ramp-up rate on module separation, as well as the separation mechanism, were investigated. In order to

eliminate the use of HF, we developed processes for chemical etching and mechanical removal to remove impurities. The validity of the process was confirmed by comparing the qualities of reclaimed wafers with those of commercial virgin wafer. A solar cell was fabricated, and its electrical properties were compared with those of the solar cell using virgin wafers.

Table 1. Various methods for removing impurities on wafer surface.

Method	Etching target	Treatment solution	Undesirable problems	Ref.
Chemical etching	ARC, p-n junction	HF + H ₂ SO ₄		9
		NH ₃ + HF + CH ₃ COOH + Br ₂		27
		HF + HNO ₃		28
		HF + HNO ₃ + H ₂ O	Acid waste, Toxic	28
		H ₂ SiF ₆ + HNO ₃ + H ₂ O		28
		H ₂ SiF ₆ + HNO ₃ + CH ₃ COOH		28
		HF, NaOH		29

Experimental

Preparation of PV module

PV modules containing multicrystalline Si solar cells (SH-1680MN, Shinsung Solar Energy, South Korea) with 156 mm × 156 mm dimensions (length and width) and 200 μm thickness were used for the study. Their initial energy conversion efficiency (Eff.) was in the range of 16.5–17.0%. The cells were interconnected by using Cu ribbon wire (2.0 mm × 0.15 mm) plated with 62Sn36Pb2Ag solder. The solar cells were laminated with low-iron glass of 3.2 mm thickness, 3.2 mm length, and 180 mm width, with an EVA sheet of 0.35 mm thickness, and with Tedlar/PET/Tedlar back-sheets of 0.35 mm thickness. The EVA sheets and back-sheets were laminated by heating them to 150 °C for 12 min.

Table 2 Test conditions of thermal process

Annealing temperature (°C)	Ramp-up rate (°C/min.)	Holding time (min.)
350, 400, 450, 480	15	30
480	5, 10, 15, 20, 30	30

Thermal process for separating the modules

PV modules were divided into two groups to investigate the effect of annealing temperature and ramp-up rate on the separation of the module. Annealing temperature is the maximum temperature for the thermal process, which is

important for determining the decomposition temperature of EVA. The thermal process was carried out with each of the two samples. PV modules were placed in a furnace (SRB30, Labtech, South Korea) and heated at the annealing temperature under ambient conditions. One group was heated to four annealing temperatures in a furnace at a fixed ramp-up rate (15 °C/min). The other group was heated to 480 °C at five ramp-up rates, as shown in Table 2. In order to quantify the ratio of unbroken wafers ($S_{i\text{ratio}}$) after the thermal process, the total weight of the sample and the largest piece of broken solar cells were measured on a digital balance (CP2245, Sartorius, Germany). Determination of the $S_{i\text{ratio}}$ is discussed below.

$$S_{i\text{ratio}}(\%) = \frac{\text{Weight of the largest solar cell piece}}{\text{Total weight of solar cell}} \times 100$$

Since the mechanical strength of a solar cell is much weaker than that of tempered glass, it is much easier for the gases to escape from the solar cell. The cell is subjected to mechanical stress caused by the gases from EVA. In order to minimize the effects of the stress on the solar cell, a fixture shown in Fig. 1 was designed and employed. Two types of load conditions were applied to the module. One group was heated with fixture (fixture) and the other without fixture (non-fixture). In case of non-fixture, the module was heated in a furnace without fixture. The figure shows a design drawing and actual images of the fixture that we employed. To release the gases, 5 mm grooves that were 5 mm apart were created. The grooves help release quickly the gases from the cell caused by EVA decomposition.

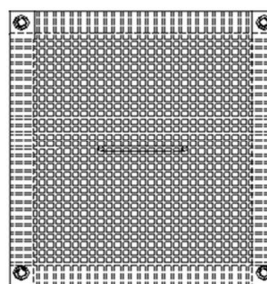
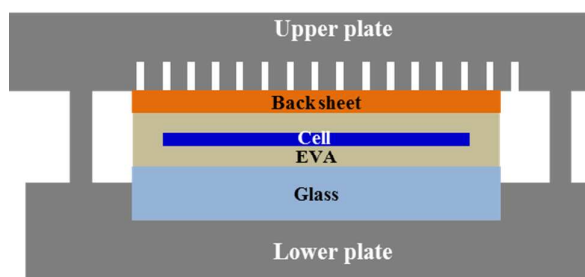


Fig. 1 Schematic images of the fixture design drawing (upper), upper plate (left), actual image (right)

Chemical etching and mechanical processes

The recovery process consisted of three steps: (1) removal of Ag electrodes using 60% nitric acid (HNO_3) at room temperature; (2) mechanical removal at 20 revolutions per minute (RPM) for 20 min using green fine silicon carbide powder (#600), which assists grinding of Si in the removal of the ARC, emitter, and p-n junction; and (3) simultaneous removal of the grinding damage on the front surface of the cell and the Al electrode from the rear side of the cells by using 45% potassium hydroxide (KOH) at 80 °C. The first etching step (HNO_3) was conducted for 120 s. Chemical etching and mechanical removal processes were performed with five samples obtained from the thermal process. To grind the front surface of the cell, the cell was affixed to a ceramic chuck and then ground on a grinding machine for 20 min at 20 RPM. The third etching step (KOH etching) was conducted for 10 min. The etching steps were carried out under conditions optimized through previous experiments.³⁰ A schematic of the processes is shown in Fig. 2.

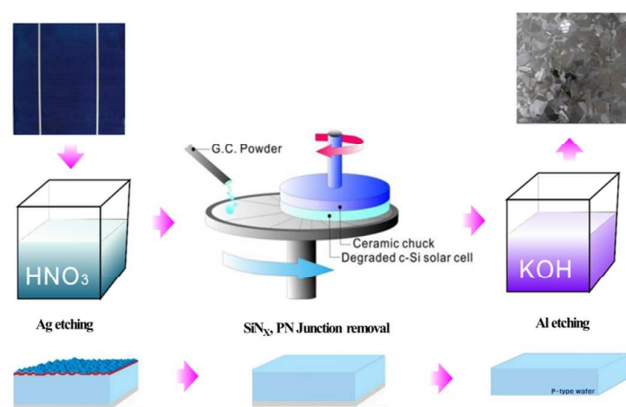


Fig. 2 Schematic diagram of a process of removing impurities remaining on the wafer surface

Characterization of reclaimed wafer

The thickness of the reclaimed wafers was measured with a digital indicator (ID-H0530, Mitutoyo, Japan). Their resistivity was measured by using a four-point probe (CMT-SR1000N, Advanced Instrument Technology, USA). Scanning electron microscopy (ESEM-FEG XL30, FEI, Holland) with energy-dispersive X-ray spectroscopy (System Six, Noran, USA) was employed to analyze the surface impurities. The concentrations of phosphorus (P) and aluminum (Al) atoms in the wafers were measured by secondary-ion mass spectroscopy (SIMS, IMS 7f, Cameca, France). Microwave detection of photoconductance decay (μ -PCD, WT-2000, Semilab) was performed to measure the carrier lifetime of the reclaimed wafers.

Fabrication of solar cells using reclaimed wafers

For surface texturing, the reclaimed wafer was dipped in an alkaline solution. To form an n+ layer structure, the wafers were treated in a tube furnace (SJ2, Sungjin-semitech, South Korea) using a POCl_3 liquid source. Phosphosilicate glass (PSG) was removed with a 10% HF solution. The SiN_x layer was deposited on the emitter by plasma-enhanced chemical vapor deposition (UT0506, Ultech, South Korea). The Ag/Al paste for the metallization process was formed by using an auto screen printer (SJI20, SJINNOTECH, South Korea) and then fired at in a lamp-heated belt furnace. The p-n junction of the cell was isolated by laser grooving. Typical characteristics of the cells at a light intensity of 1 SUN were measured by using a solar simulator (WXS-155S-L2, Wacom, Japan).

Results and discussion

The effect of annealing temperature on module separation

Fig. 3 shows that the Si_{ratio} increased with annealing temperature. However, the Si_{ratio} in the case of nonfixture was below 5% at all annealing temperatures. We achieved 100% Si_{ratio} when we annealed the module for 30 min at 480 °C, which is the end point of the second decomposition of EVA.³¹

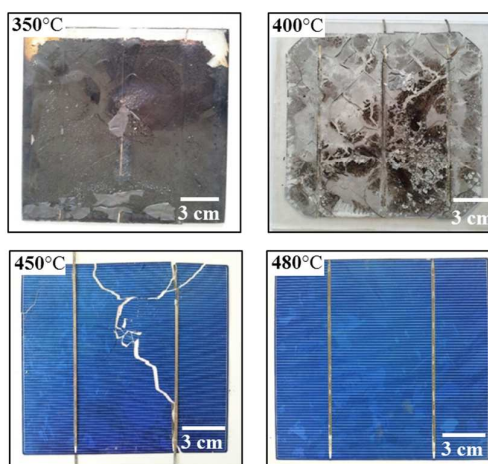
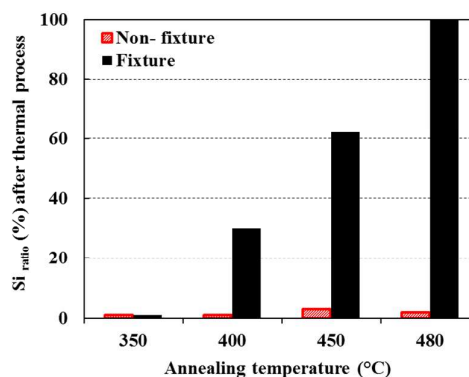


Fig. 3 Unbroken wafer ratio with and without fixture (upper) and image (lower) after thermal process at a fixed ramping-up

rate of 15 °C/min with fixture. Four kinds of temperatures were applied for annealing: 350, 400, 450 and 480 °C

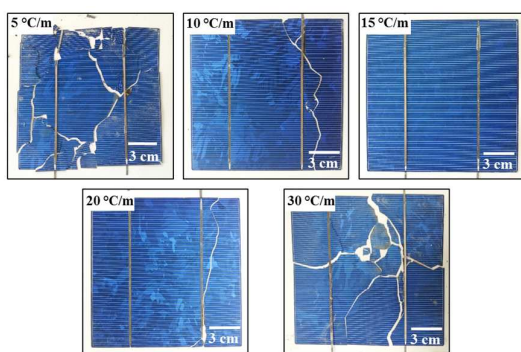
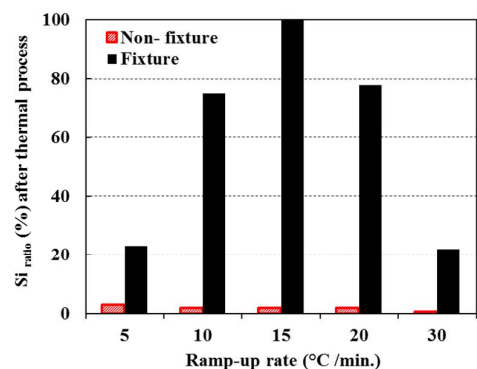


Fig. 4 Unbroken wafer ratio with and without fixture (upper) and image (lower) after thermal process at 480 °C with fixture. Five kinds of ramping-up rates were applied: 5, 10, 15, 20, 30 °C/min.

Although EVA was completely separated from the solar cells when we annealed the module at 450 °C, some cracks formed in the cell and thus decreased the Si_{ratio} to 60%. Below 450 °C, the EVA sheet and back-sheet did not fully decompose and were thus inseparable from the solar cells.

The effect of ramp-up rate on the Si_{ratio} is shown in Fig. 4. The figure shows that the Si_{ratio} reached 100% at 15 °C/min. However, in the case of nonfixture, the Si_{ratio} was below 5% at all ramp-up rates. At rates higher or lower than 15 °C/min, the Si_{ratio} decreased. At low ramp-up rates, however, various parts of the solar cells were damaged.

Weight-loss behaviors of the EVA sheet and back-sheet (Fig. 5) were analyzed by thermogravimetric analysis (TGA-4000, Perkin Elmer, USA). The EVA sheet and back-sheet lost weight through various steps. EVA experienced 30 and 90% weight loss at 370 and 480 °C, respectively.

Primary decomposition from 260 °C to 370 °C released acetic acid at this stage.³² Second decomposition occurred from 370 °C to 480 °C. Initiation reactions in the second decomposition involve scission of tertiary carbon bonds or

ordinary carbon-carbon bonds in the beta position relative to tertiary carbons. The major products of decomposition are propane, propene, ethane, butene, hexene-1, and butene-1.³¹

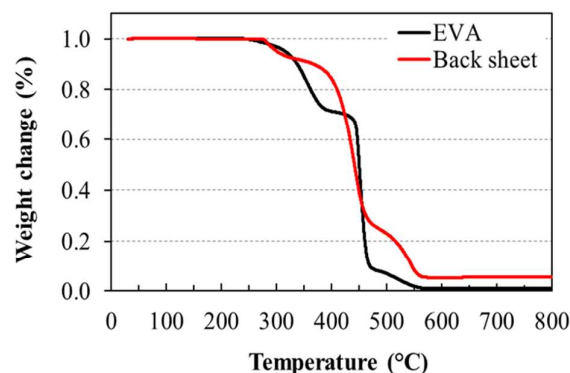


Fig. 5 Weight loss of EVA and back-sheet as a function of temperature

These gases may be removed by appropriate equipment such as an electrostatic precipitator or a fabric filter.³³ The results demonstrate that EVA decomposition was nearly completed at 480 °C. The back-sheet lost 10, 30, and 95% of its weight at 370, 480, and 560 °C, respectively. EVA resembles a gel and remains stable at low ramp-up rate. EVA in gel-like form continuously emits gases, steadily producing mechanical stress in the cells and initiating cracks at weaker parts of the cells, which eventually spread out. Therefore, careful control of the ramp-up rate is necessary.

The major cause of cell breakage is the gases generated by EVA decomposition.³¹ These gases accumulate between EVA and back-sheet. EVA is much less likely to damage the cells because it is easier for the gases to escape through the back-sheet as it decomposes; this process leads to more escape pathways for the gases. However, the gases between the cell and glass can affect cell breakage. According to TGA analysis, the first decomposition of both the back-sheet and EVA started at about 260 °C. The gases in this stage escape through

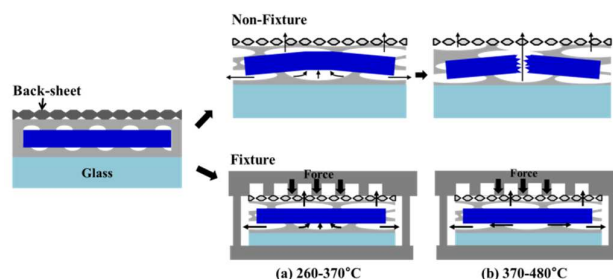


Fig. 6 Module separation procedures during thermal process. Cell breakage process (upper) in case of non-fixture and

mitigation method (lower) of cell breakage by using fixture during thermal process

the EVA sheet and back-sheet (Fig. 6(a)) or become trapped between the glass and cell. As the temperature increases, the decomposition of the back-sheet and EVA accelerates, and gas generation accelerates.³¹ The gases result in a high pressure between cell and glass and tend to occupy the cell (Fig. 6(b)), leading to cell breakage in the case of non-fixture. Application of force to the cell prevents release of the gases from cell, as shown Fig. 6. In addition, in order to obtain a cell that has no crack, it is important to draw gases from EVA and back-sheet out. If there are no grooves at the upper plate, the gases have to move through the gap between upper plate and back-sheet. However, the residue after decomposition makes the gases difficult to escape. The gases trap between cell and fixture. It makes stresses between cell and fixture, which result in the crack of the cell. Therefore, the grooves in the fixture help the gases released from EVA and back-sheet to escape effectively. This result suggests that the Si solar cell may be separated from the module without damage when the proper load is applied.

The results of chemical etching and mechanical processes

The first step of the recovery process is removal of Ag electrodes on the front surface of the cell. The electrodes may be removed with the ARC, emitter, and p–n junction by mechanical removal. This one-step process can thus make the recovery process more simple and efficient. However, we employed HNO₃ etching for two reasons: (1) prevention of cracks on wafers due to the height difference between the top of the Ag electrodes and the top of the wafer surface and (2) recovery of Ag from the Ag electrode. As the Ag electrode stands high above the wafer surface, cracks can form on the front surface of the wafer when a grinding wheel presses down on the wafer.

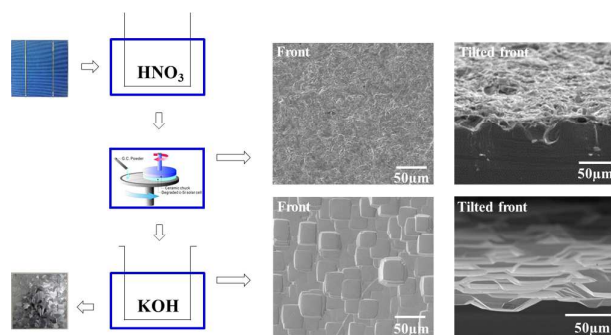


Fig. 7 SEM images of the front surface of the wafer after mechanical removal (upper), and after KOH etching (lower)

In addition, recovering Ag from the front electrode before grinding is more convenient than recovering it from wastes

after mechanical grinding. This is because of the process required to recover Ag from wastes after grinding. For these reasons, HNO₃ etching process was employed for the first etching process. This reaction may generate toxic fumes of nitric acid, which has significant effects on the environment, such as acid rain and photochemical smog,³⁴ as well as harmful effects on human health. Therefore, this process must be conducted in the fume hood. In addition, the waste after mechanical removal can be used as raw material for silicon refining.³⁵

Fig. 7 shows a SEM image of the top surface of the ground wafer subjected to HNO₃ etching and mechanical removal. The figure shows that the wafer surface is uneven. The roughness is caused by green silicon carbide fine powder, which was used to make grinding efficient. However, it left grinding damage on the front surface of the cell. This damage may be removed by KOH etching process,³⁶ which simultaneously etches the Al rear contact. The mechanical process enabled removal of impurities on the cell surface. Our previous study³⁰ even used 3 liters of 49% HF solution to remove impurities for 50 Si solar cells. This process decreased the total amount of chemicals used in the present study of 50% relative to that in our previous research (Table 2).³⁰

Table 2. Type and amount of chemicals used in previous and current research.

Chemical	Our previous research ³⁰			Current method		
	49%	60%	90%	49%	60%	30%
Amount	3 L	11 L	14 L	N/A	7 L	7 L

Fig. 7 also shows the front surface of the wafer subjected to KOH etching followed by the mechanical removal process. The purpose of this process is to remove the Al rear contact, back surface field, and grinding damage caused by the grinding process. As seen in the figure, the front surface after KOH etching was uniform. The surface of the wafer was nearly identical to that of a commercial wafer after saw damage removal process using KOH. Therefore, grinding damage was removed thoroughly by the etching process. In order to dispose KOH liquid which was generated during Al etching, we added H₂SO₄ to KOH liquid wastes to form Al(OH)_{3(s)} and K₂SO_{4(aq)}. Subsequently, Al(OH)_{3(s)} and K₂SO_{4(aq)} were separated by filtering, and then Al(OH)₃ was heated to form Al₂O₃.³⁷ Table 3 lists the final thickness and resistivity of the reclaimed wafers after KOH etching. In order to apply current fabrication processes for crystalline-Si (c-Si) solar cells, securing a suitable final thickness of reclaimed wafers is important. Therefore, we sought to achieve a final thickness of 170–180 μm for the reclaimed wafers. As can be seen in Table 3, the average final thickness of the reclaimed wafers was approximately 180 μm. Since the thickness could be controlled by mechanical removal, the reclaimed wafers showed nearly the same final thickness. These results indicate that the recovery process has high reproducibility and accuracy.

One of the important properties of initial wafers is their resistivity. To evaluate the quality of the reclaimed wafers, we measured their resistivity and compared it with the resistivity of virgin wafers. The minimum and maximum resistivities of the reclaimed wafers were 0.6 and 3.7 $\Omega\cdot\text{cm}$, respectively. The average resistivity of commercial virgin wafers lies in the range of 0.5–3.0 $\Omega\cdot\text{cm}$. Therefore, the resistivity of the five reclaimed wafers was close to that of commercial virgin wafer. SIMS analysis was conducted to determine the P concentration on the front and the Al concentration on the rear side of the reclaimed wafers. In most commercialized c-Si solar cells, P atoms diffuse to the front surface of the p-type wafer to form a p–n junction and an emitter layer. Therefore, we can verify whether mechanical removal thoroughly removes the emitter layer by measuring the concentration of P atoms on the front surface of the cells.

Table. 3 Thickness and resistivity of reclaimed wafers after chemical and mechanical processes (Thickness tolerance is $\pm 10 \mu\text{m}$)

	Commercial	#1	#2	#3	#4	#5
Thickness(μm)	200	180	180	179	179	179
Resistivity ($\Omega\cdot\text{cm}$)	0.5–3.0	0.6–3.7	1.3–2.7	0.8–1.4	0.9–2.3	1.5–3.1

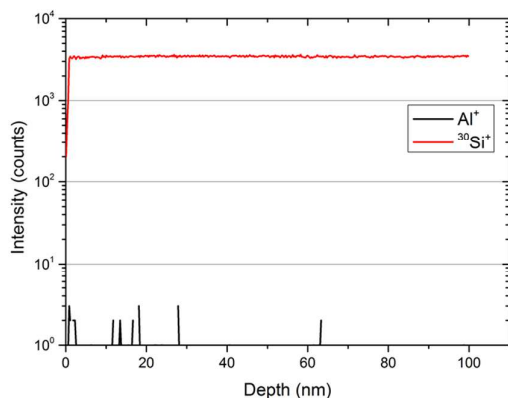
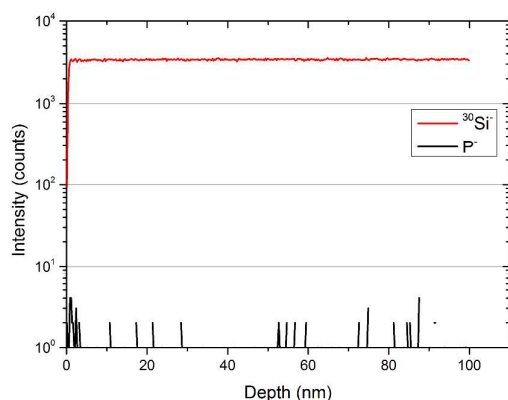


Fig. 8 SIMS analysis results P concentration on the front surface (upper) and Al concentration on the rear surface of the reclaimed wafer (lower)

Similarly, the concentration of Al atoms on the rear surface may be measured to determine whether the Al rear electrode and back surface field (BSF, barrier block minority carriers that flow to the rear contact) are perfectly etched. To make a reclaimed wafer from the solar cell, the emitter, p–n junction, Al rear electrode, and BSF must be removed. This requirement means that P and Al atoms should not be detected by SIMS measurements.

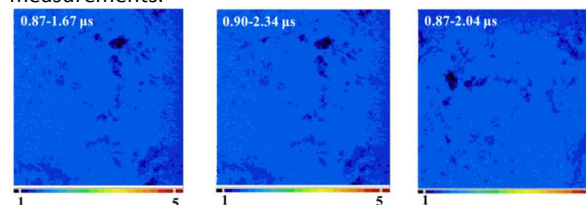


Fig. 9 Images of carrier lifetime of reclaimed wafers.

Top and bottom panels of Fig. 8 respectively show the P concentration on the front surface and the Al concentration on the rear surface of the reclaimed wafers. They indicate that throughout the penetration depth of the wafer, P and Al atoms were hardly detectable on the front and rear surfaces, respectively. Therefore, the emitter layer, p–n junction, Al rear electrode, and BSF were completely removed by the combined mechanical removal and chemical etching process.

The carrier lifetime of the reclaimed wafers was measured and then compared with that of commercial virgin wafer. The carrier lifetime of most commercial solar-grade crystalline wafers without any surface passivation is in the range of 0.5–3 μs .³⁸ Mapping results for the carrier lifetime for the reclaimed wafers (Fig. 9) show that the carrier lifetime of the reclaimed wafers is in the range of 0.87–2.34 μs , which is close to that of commercial wafers.



Fig. 10 Image of an reclaimed wafer obtained by the recovery processes (left) and remanufactured solar cell with reclaimed wafer (right).

Fig. 10 (left) shows an image of the final reclaimed wafer. The obtained reclaimed-wafer had a smooth and uniform surface and resembled a commercial virgin wafer. We fabricated Si solar cells using reclaimed wafers, as shown in Fig. 10 (right). The initial Eff. value is in the range of 16.5–17.0%. Even if the Eff. of Si solar cells varied with the structure, fabrication method, and manufacturing recipe, we achieved 16.6–16.9% Eff. by using the reclaimed wafers.

Conclusions

In the present study, we demonstrated processes to obtain reclaimed wafers from PV modules. We applied a thermal process to remove EVA and the back-sheet, and we found that the gases released from EVA decomposition during the process damaged the wafers in the PV module. To prevent the damage, we designed and employed a fixture to release the gases. Various ramp-up rates and annealing temperatures were tested to obtain the highest $S_{i\text{ratio}}$. We achieved 100% $S_{i\text{ratio}}$ at 15 °C/min and at an annealing temperature of 480 °C, which is the end point of the second decomposition of EVA and the back-sheet. We also developed a method for removing impurities, which we combined with mechanical removal and chemical etching. To obtain reclaimed wafers from the separated cells, Ag and Al metal electrodes were etched with HNO_3 and KOH respectively. The ARC, emitter layer, and p–n junction were removed mechanically. After the mechanical process, the front surface of the cell was damaged; however, it was removed during the KOH etching process. We were thus able to achieve a uniform and smooth surface. The final thickness of the reclaimed wafers was 180 μm , which is sufficient for use in current processes for solar cells. In addition, the minimum and maximum resistivities of reclaimed wafers were 0.6 and 3.7 $\Omega\cdot\text{cm}$, respectively, and their lifetime was 0.87–2.34 μs . These values are almost equal to those for commercial virgin wafers. Finally, we applied a standard manufacturing process for Si solar cells using the reclaimed wafers and achieved an Eff. value of 16.6–16.9%.

Acknowledgements

This work was supported by the Korea Evaluation Institute of Industrial Technology (KEIT) grant funded by the Ministry Of Trade, Industry & Energy (MOTIE), Republic of Korea (No. 10044920).

Notes and references

The authors in this paper, Jongsung Park and Wangou Kim contributed equally to this work.

1. I. PVPS, 2015.
2. E. P. I. Association, *Publications/44_epia_gmo_report_ver_17_mr.pdf*, 2014.
3. C. Sener and V. Fthenakis, *Renewable and Sustainable Energy Reviews*, 2014, **32**, 854–868.
4. J.-K. Choi and V. Fthenakis, *Journal of Cleaner Production*, 2014, **66**, 443–449.
5. A. Paiano, *Renewable and Sustainable Energy Reviews*, 2015, **41**, 99–112.
6. Y. Qu, Q. Zhu, J. Sarkis, Y. Geng and Y. Zhong, *Journal of Cleaner Production*, 2013, **52**, 176–184.
7. F. Cucchiella and P. Rosa, *Renewable and Sustainable Energy Reviews*, 2015, **47**, 552–561.
8. J. Clynck, *IEA PVPS TASK 12 Workshop*, 2015.
9. S. Kang, S. Yoo, J. Lee, B. Boo and H. Ryu, *Renewable Energy*, 2012, **47**, 152–159.
10. M. Marwede, W. Berger, M. Schlummer, A. Mäurer and A. Reller, *Renewable Energy*, 2013, **55**, 220–229.
11. A. Gölle, P. Görbe and A. Magyar, *Journal of Cleaner Production*, 2012, **34**, 138–145.
12. J. R. Dodson, H. L. Parker, A. M. García, A. Hicken, K. Asemave, T. J. Farmer, H. He, J. H. Clark and A. J. Hunt, *Green Chemistry*, 2015, **17**, 1951–1965.
13. E. Bombach, A. Müller, K. Wambach and I. Röver, in *20th European Photovoltaic Solar Energy Conference, Barcelona*, 2005.
14. M. L. Bustamante and G. Gaustad, *Applied Energy*, 2014, **123**, 397–414.
15. A. J. Hunt, A. S. Matharu, A. H. King and J. H. Clark, *Green Chemistry*, 2015, **17**, 1949–1950.
16. P. Wu, B. Xia and X. Zhao, *Renewable and Sustainable Energy Reviews*, 2014, **37**, 360–369.
17. ITRPV, International technology roadmap for photovoltaic, 2015.
18. E. Bombach, I. Röver, A. Müller, S. Schlenker, K. Wambach, R. Kopecek and E. Wefringhaus, in *21st European Photovoltaic Solar Energy Conference*, 2006, pp. 4–8.
19. J. Zhang, F. Lv, L. Y. Ma and L. J. Yang, *Advanced Materials Research*, 2013, **724**, 200–204.
20. J. C. Marchal, D. J. Krug III, P. McDonnell, K. Sun and R. M. Laine, *Green Chemistry*, 2015, **17**, 3931–3940.
21. A. Müller, K. Wambach and E. Alsema, in *MRS Proceedings*, Cambridge Univ Press, 2005, pp. 0895–G0803–0807.
22. L. Frisson, H. Hofkens, K. De Clercq, J. Nijs and A. Geeroms, *status: published*, 1998, 2210–2213.
23. M. M. de Wild-Scholten, *Solar energy materials and solar cells*, 2013, **119**, 296–305.
24. M. Goe and G. Gaustad, *Applied Energy*, 2014, **120**, 41–48.
25. G. Granata, F. Pagnanelli, E. Moscardini, T. Havlik and L. Toro, *Solar Energy Materials and Solar Cells*, 2014, **123**, 239–248.
26. L. Frisson, K. Lieten, T. Bruton, K. Declercq, J. Szlufcik, H. De, M. Goris, A. Benali, O. Aceves and S. Kapeldreef, 2000.
27. E. Klugmann-Radziemska, P. Ostrowski, K. Drabczyk, P. Panek and M. Szkodo, *Solar energy materials and solar cells*, 2010, **94**, 2275–2282.
28. E. Klugmann-Radziemska and P. Ostrowski, *Renewable energy*, 2010, **35**, 1751–1759.
29. T.-Y. Wang, J.-C. Hsiao and C.-H. Du, in *Photovoltaic Specialists Conference (PVSC), 2012 38th IEEE*, IEEE, 2012, pp. 002355–002358.
30. J. Park and N. Park, *RSC Advances*, 2014, **4**, 34823–34829.

Journal Name

ARTICLE

31. C. L. Beyler and M. M. Hirschler, *SFPE handbook of fire protection engineering*, 2002, **2**.
32. M. Marin, A. Jiménez, J. López and J. Vilaplana, *Journal of thermal analysis*, 1996, **47**, 247-258.
33. M. Tamaro, J. Rimauro, V. Fiandra and A. Salluzzo, *Renewable Energy*, 2015, **81**, 103-112.
34. Z. Liu, J. Hao, L. Fu and T. Zhu, *Applied Catalysis B: Environmental*, 2003, **44**, 355-370.
35. J.-K. Lee, J.-S. Lee, B.-Y. Jang, J.-S. Kim, Y.-S. Ahn, G.-H. Kang and C.-H. Cho, *Journal of Nanoscience and Nanotechnology*, 2015, **15**, 8547-8552.
36. H. Seidel, L. Csepregi, A. Heuberger and H. Baumgärtel, *Journal of the electrochemical society*, 1990, **137**, 3612-3626.
37. S. Hashimoto and A. Yamaguchi, *Journal of the European Ceramic Society*, 1999, **19**, 335-339.
38. K. Bothe, R. Krain, R. Falster and R. Sinton, *Progress in Photovoltaics: Research and Applications*, 2010, **18**, 204.